Three-dimensional morphometry of spinal cord injury following polyethylene glycol treatment

Bradley S. Duerstock and Richard B. Borgens*

Center for Paralysis Research, Institute for Applied Neurology, Department of Basic Medical Sciences, School of Veterinary Medicine, Purdue University, West Lafayette, IN 47907-1244, USA

*e-mail: cpr@vet.purdue.edu

Summary

We are developing a novel means of restoring function after severe acute spinal cord injury. This involves a brief application of polyethylene glycol (PEG) to the site of injury. In the companion paper, we have shown that a delayed application of PEG can produce strikingly significant physiological and behavioral recovery in 90–100 % of spinal-cord-injured guinea pigs. In the present paper, we used three-dimensional computer reconstructions of PEG-treated and sham-treated spinal cords to determine whether the pathological character of a 1-month-old injury is ameliorated by application of PEG. Using a novel isocontouring algorithm, we show that immediate PEG treatment and treatment delayed by up to 7 h post-injury statistically increased the volume of intact spinal parenchyma and reduced the amount of cystic cavitation. Furthermore, in PEG-treated animals, the lesion was more focal and less diffuse throughout the damaged segment of the spinal cord, so that control cords showed a significantly extended lesion surface area. This three-dimensional computer evaluation showed that the functional recovery produced by topical application of a hydrophilic polymer is accompanied by a reduction in spinal cord damage.

Key words: three-dimensional reconstruction, computer visualization, morphometry, spinal cord injury, neurotrauma, cavitation.

Introduction

Polyethylene glycol (PEG) is a hydrophilic polymer that has been used for many years to fuse the membranes of various types of cell to produce hybridomas, as a model for vesicular fusion (Davidson et al., 1976; Nakajima and Ikada, 1994; Lee and Lentz, 1997), and to achieve fusion of neurons and single giant axons in invertebrates (O'Lague and Huttner, 1980; Krause and Bittner, 1990). Our laboratory has shown that PEG can be used to effect an anatomical and functional reconnection of transected axons of guinea pig spinal cord white matter maintained in isolation (Shi et al., 1999). We have also reported the 'rescue' of nerve impulse conduction in severely crushed guinea pig spinal cord maintained in a novel isolation and recording chamber (Shi and Borgens, 1999). More recently, this same topical PEG application has been used to produce rapid behavioral and physiological recovery from a standardized spinal cord injury in adult guinea pigs. Behavioral function was determined using a spinal-cord-dependent long-tract reflex, the cutaneous trunci muscle (CTM) reflex, as an index of white matter integrity (Borgens and Shi, 2000). In our companion paper (Borgens et al., 2002), we have focused on a 7 h delayed application, showing that application of PEG still leads to the recovery of behavioral function in over 90 % of the treated population.

It is believed that more extensive damage to the spinal cord occurs with time after the initial trauma by a progressive and delayed 'secondary injury' process (Blight, 1992, 1993; Honmou and Young, 1995). Since the application of PEG rescues significant behavioral and physiological function in every animal treated, we believed this would be associated with a considerable rescue of spinal cord parenchyma through the sealing of damaged cell membranes. This idea was tested in the present study using histological data sets obtained from animals that were part of the study of the delayed application of PEG (Borgens et al., 2002) as well as an equivalent number of animals obtained from studies of the immediate application of PEG following injury (Borgens and Shi, 2000).

The injury site of the chronically traumatized mammalian spinal cord is located predominantly in the central regions of the spinal cord, making three-dimensional anatomical description of the lesion difficult. Previous histological techniques have required the investigator to infer three-dimensional morphology from a series of two-dimensional sections. In addition, measuring these three-dimensional structures from serial sections has required the use of two-dimensional morphometry or other approximation methods (Blight, 1985; Noble and Wrathall, 1985; Harris and Stevens, 1988; Hashimoto and Kimura, 1988; Bresnahan et al., 1991; Halliday et al., 1993; Arndt et al., 1994; Navarro et al., 1994;

Salisbury, 1994). Here, we applied novel three-dimensional algorithms to generate computer models of the injured spinal cord developed from complete sets of the serial histological sections comprising a spinal cord segment containing the lesion. This software allowed the visualization of the three-dimensional shape and pathological structures of injured cords and, to our knowledge, is the only means of measuring the surface area and volume of pathological features of interest from the reconstruction itself (Duerstock et al., 2000). These new computer reconstruction techniques have already proved to be ideal for morphometrical evaluation of complex histological material (Moriarty et al., 1998).

Since 100 % of the control (untreated) population failed to recover conduction through the compression lesion, while 100 % of the PEG-treated animals recovered conduction swiftly, and since 93 % of PEG-treated animals recovered behavioral function compared with infrequent spontaneous recovery in controls, it was likely that every PEG-treated spinal cord would be markedly different from sham-treated spinal cords in other aspects of evaluation. Thus, data sets from four animals from an 'immediate' PEG-treated group and six animals from a 'delayed' PEG-treated group were reconstructed and compared with a set of four control animals. We found that PEG application statistically significantly increased the amount of spared parenchyma in injured spinal cords while also significantly reducing the degree of cavitation and cyst formation.

Materials and methods

The sets of serial histological sections were chosen from studies in which guinea pigs had received the same standardized spinal cord injury and (i) an immediate application of PEG (Borgens and Shi, 2000), (ii) or the associated control applications where water ('vehicle') was applied immediately after injury (Borgens and Shi, 2000) or (iii) a delayed application of PEG (Borgens et al., 2002). We briefly review the procedures applied to all animals below.

Animals

Adult (300 g) laboratory guinea pigs were used in these experiments. Following surgery (see below), they were housed two animals per cage and fed *ad libitum*; their health was monitored daily. Seventeen animals in this study were killed 1 month post-treatment by anesthetizing them with 0.2 ml of ketamine HCl and 0.2 ml of xylazine, then by an overdose of sodium pentobarbital (0.8 ml of $1\,g\,ml^{-1}$ standard injectable) immediately followed by perfusion/fixation with 6 % paraformaldehyde, 0.5 % glutaraldehyde in phosphate buffer. Segments of spinal cord containing the injury sites were dissected free and immersion-fixed in the above fixative for approximately 18 h.

Surgical procedures

Anesthesia was performed using an intramuscular injection of 0.1 ml $100\,g^{-1}$ body mass of a standardized solution of $100\,mg\,kg^{-1}$ of ketamine HCl and $20\,mg\,kg^{-1}$ of xylazine. The spinal cord was exposed by a partial laminectomy (between the tenth and twelfth thoracic vertebrae), the dura was removed with sharpened watchmakers' forceps and the dorsal hemisphere was compressed for 15 s using blunted watchmakers' forceps possessing a détente to standardize the displacement of the spinal cord (Blight, 1991; Moriarty et al., 1998). For five spinal cords in one experimental group, PEG (M_r 1800, 50 % w/v in water) was applied to the injury site with a pipette immediately after the crush. The injury site was rinsed after 2 min with Krebs' solution to remove the PEG. In a second experimental group consisting of seven spinal cords, PEG was applied approximately 7 h post-injury before being rinsed off. In sham-treated control animals, water ('vehicle') was immediately applied to the lesion for 2 min and aspirated. The injury site was then lavaged with Krebs' solution. Surgical incisions were closed in layers with 3-0 proline suture, and the skin was closed with wound clips. Immediately post-surgery, each animal was injected subcutaneously with 3 ml of lactated Ringer's solution to prevent dehydration, and the animal was placed under a heat lamp for approximately 24 h to reduce post-surgical mortality due to shock.

Histological preparation

The excised segments of spinal cord (approximately one vertebral segment; approximately 1 cm in length) including the experimental injury were dehydrated in ascending concentrations of alcohol followed by xylene to allow infiltration and embedding in Paraplast (paraffin) by conventional methods. This piece of cord was reduced in length by removing undamaged tissue at the rostral and caudal ends, yielding a segment length of approximately 4.2 mm containing the lesion in its center. This shorter segment facilitated histological sectioning and the retrieval of these serial sections. Even minor imperfections in the retrieved sections (that would be of little consequence to two-dimensional evaluation and morphometry) can spoil the precision of the three-dimensional registration and reconstruction process.

This entire cord segment was then sectioned on a rotary microtome at approximately 15 μm per section, and horizontal longitudinal sections were affixed to microscope slides. Prior to use, the slides were dipped in a 0.5 % (w/v) gelatine solution that aids the adhesion of the sections to the slides during subsequent treatment. Paraffin was partially removed with a 1 h treatment in an oven at 60 °C and completely removed after a 1 h immersion in 100 % xylene. Sections were rehydrated by immersions in descending concentrations of alcohol in distilled water using conventional methods. All sections were stained with Holme's silver stain, counterstained with Neutral Red and coverslipped in Permount. The silver stain clearly revealed intact white and gray matter, while the counterstain delineated the region of central hemmorhagic necrosis. Cysts were revealed by the absence of stain.

Video capturing and registration of serial sections

An Optronics DEI-750 color video camera mounted on an Olympus Van Ox Universal microscope displayed histological
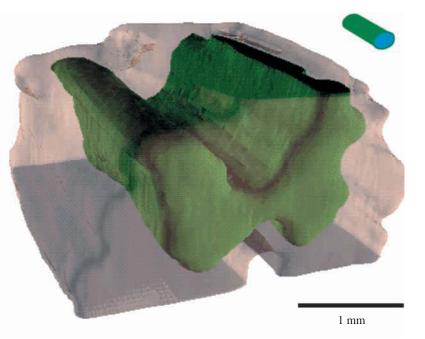
Fig. 1. Three-dimensional reconstruction of a normal spinal cord segment. An uninjured spinal cord segment was reconstructed using the isocontouring method to demonstrate that a familiar, normal morphology is reproduced. This serves as an image 'control' or reference for the reader since spinal cord injury produces an unfamiliar, unusually stenotic, and misshapen structure. The white matter was made transparent while the central gray matter was rendered in green in this visualization. The dorsal and ventral surfaces are flat because these very small sections (cutting into and out of the tissue block) were usually lost or damaged. In this and subsequent figures, the cylindrical icon indicates the relative orientation of the three-dimensional segment. The blue color indicates the caudal end of the cylinder. Unless noted otherwise, the dorsal surface of all reconstructed spinal cords faces towards the top of the page.

1 mm

sections on a computer monitor. Histological images were then acquired to a dual Pentium Pro computer using Adobe Photoshop software and managed on a Silicon Graphics Indigo for three-dimensional surface reconstruction. Registration was performed by superimposing each successive histological section by optimally positioning and rotating the microscope stage onto a tracing of the previously captured image made on the computer monitor. The boundaries of the spinal cord, cysts and lesion site served as effective fiducial markers.

Three-dimensional reconstruction

As mentioned above, all retrieved histological sections obtained from these spinal segments were used during three-dimensional reconstruction. Only a few of the most dorsal and ventral sections were lost as the microtome advanced into and out of the tissue. This minor loss of sections made the reconstructed images appear flattened on their most dorsal and ventral surfaces (see below). Serial histological sections must be in excellent condition to permit effective registration and/or reconstruction. For this reason, one spinal cord data set was chosen, and deleted, from each of the three groups (control, immediate PEG application and delayed PEG application) that was not of the quality of the remaining sets. This gave a final set of four control, four immediate PEG application and six delayed PEG application spinal cord.

The isocontouring algorithm proposed by Bajaj et al. (1997) was used for all three-dimensional reconstruction. We chose this novel three-dimensional reconstruction algorithm rather than commercially available software to image the spinal cord injuries three-dimensionally because of its ease of use and ability to interrogate reconstructed samples and objects embedded within the samples quantitatively (Duerstock et al., 2000). For, reference, Fig. 1 demonstrates the ability of the isocontouring method to produce an effective three-dimensional image of an undamaged spinal cord segment from serial histological sections.

The isocontouring method

The isocontouring method employs a spectral interface to select the voxel value or 'isovalue' of the regions of the spinal cord tissue to be displayed as a three-dimensional image. Choosing which isovalue to use for three-dimensional reconstruction can be biased if the user looks only at the final three-dimensional image to determine conformation. Therefore, we used a visual spectrum analysis of the three-dimensional data sets to select distinct structures of the spinal cord injury and to maintain uniformity during isovalue selection for all spinal cord reconstructions (Bajaj et al., 1997). Isovalues were chosen at distinct features on the visual spectrum that indicated the presence of prominent surfaces in the data set.

All computer capture of data sets was performed on sections given an identification code by a technician. The identity of all spinal cord data sets (control, immediate PEG application or delayed PEG application) was unknown to the investigators. One investigator (BD) was also blind to the identity of experimental and control spinal cord injuries during isovalue selection, as mentioned above, and subsequent production and quantitative interrogation of the three-dimensional image. The identity of none of the images was revealed until all three-dimensional visual images had been finalized, quantitatively queried and the numerical data organized in spreadsheets.

Three-dimensional morphometric analysis

We measured regions of intact spinal cord parenchyma, lesion formation and cavitation on the basis of differences in their pixel density in both PEG-treated and sham-treated spinal cords. Intact white matter appeared dark red to reddish/black at low magnification because of the black staining of axons set against a Neutral Red counterstain. The lesion could be identified by its pale staining since it was devoid of Holme's-silver-impregnated neurons and axons (Fig. 2).
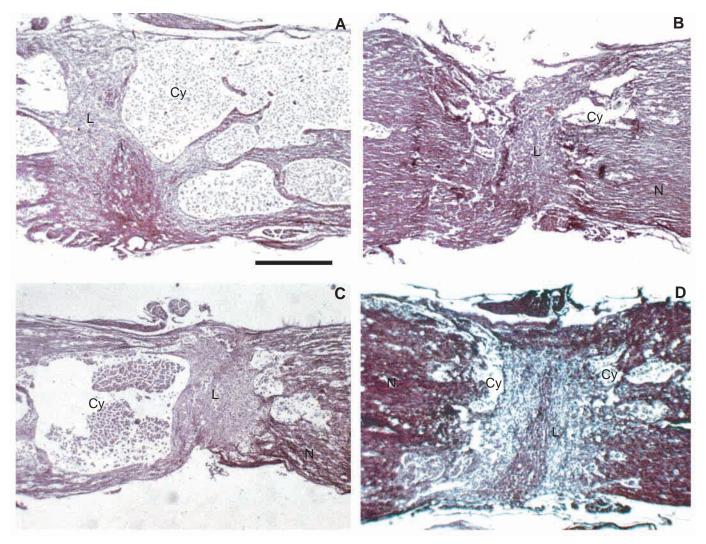
Fig. 2. Histological sections of the lesion in PEG-treated and untreated spinal cords. Typical horizontal/longitudinal histological sections acquired to computer for three-dimensional reconstruction. All views shown were obtained from histological sections at the epicenter or most extensively damaged region of the lesion. A and C are typical of untreated (control) spinal cord lesions, while B and D are representative of those treated with PEG. Note the extensive cystic cavitation in control cords and the relative absence of cavitation in the PEG-treated spinal cords. In A and C, the rostral/caudal extents of the cysts are beyond the boundaries of the image. N, intact spinal cord parenchyma; L, lesion; Cy, cysts. The rostral end is to the left in all images. Scale bar (for A–D), 1 mm.

We calculated the size (area or volume) of cysts by subtracting the size of healthy and necrotic tissue (Figs 2, 3B) from the size of the complete spinal cord segment (Figs 2, 3A). The size of the lesion was calculated by taking the total quantity of nervous tissue without cysts (Figs 2, 3B) and subtracting the measurements of undamaged spinal cord parenchyma (Figs 2, 3C). Some of the numerical data, particularly the lesion surface area in the PEG-treated groups, resulted in a negative value if the surface area of the undamaged parenchyma was greater than the surface area of the total spinal cord tissue.

To account for the varying size of spinal cord segments, we normalized the measurements of volume or surface area by dividing each feature of interest by the volume or surface area of that spinal cord segment and multiplying by 100. This gives a percentage of the total volume or surface area of an anatomical feature of interest relative to the spinal cord segment containing it.
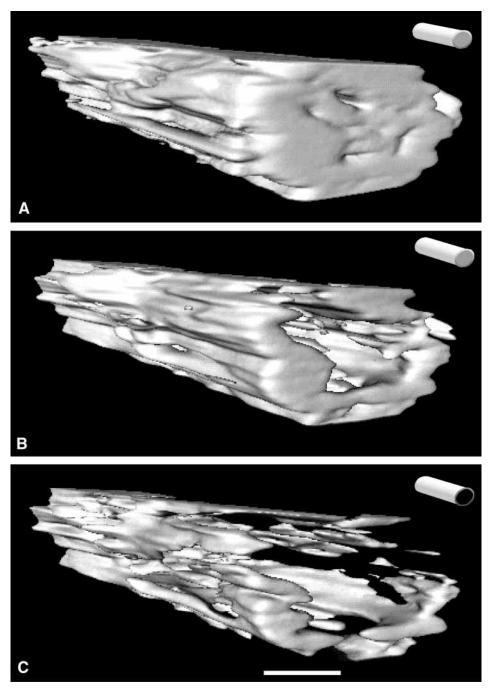
Statistical evaluation

The acceptable use of a small sample size from each comparator (treatment) group was described above. We further substantiated this number of subjects by using a one-tailed, Student's t-distribution equation:

$$N = 2 \left[\frac{S(t_{2\alpha} + t_{2\beta})}{\theta} \right]^2,$$

where S is standard deviation, $\alpha=\beta=0.1$ and θ (the success criterion) is 30 % or greater. Fewer than four subjects are required in each comparator group, which is below the sample size we used, to reach statistical significance.

Fig. 3. Quantitative querying of three-dimensional reconstructions. By selecting different isovalues, specific structures of interest can be imaged three-dimensionally (refer to Materials and methods). In A, the 4.2 mm length of reconstructed control spinal cord is shown containing the entire region of damaged spinal cord, including cysts and lesioned parenchyma. The three-dimensional visualization algorithm also allowed the surface area and volume of this structure to be determined. The shape of the segment is compacted because of compression injury, although the flattened dorsal and ventral surfaces are artifacts arising from the loss of a few histological sections during sectioning as explained in Fig. 1 and in Materials and methods. In B, the intact and damaged parenchyma of the spinal cord segment are shown without the cystic cavitations, which could be imaged separately (by isovalue selection) and deleted from the overall reconstruction. Note the presence of a large cyst extending from the center of the rostral end of the segment (facing the viewer) as a pocket within the spinal cord. The surface area and volume of the cysts were easily calculated by subtracting numerical values obtained from this reconstruction (B) from those obtained from the section shown in A. (C) The intact spinal cord parenchyma, which was also evaluated quantitatively. Note that most of the spared parenchyma is found at the periphery of the spinal segment. Numerical values derived from this reconstruction (C) were subtracted from those for B to give the surface area and volume of the lesion. The cylindrical icon gives the relative orientation of the three-dimensional segment; gray is the rostral end and black is the caudal end. Scale bar (for A–C), 1 mm.

The normalized measurements of the three-dimensional reconstructions between control and experimental groups were compared using an unpaired, two-tailed, Student's *t*-test. Pearson correlation tests were used to test linear relationships. Computations were performed using Instat software.

Results

Three-dimensional imaging of the reconstructed spinal cords

The compression injury was extremely severe and resulted in spinal cord segments with a rough and clearly compressed external appearance. The site of compression was evident as a bilateral indentation of the spinal cord segment sometimes giving it an hourglass appearance (Fig. 2B–D). Curiously, spinal cord segments containing many cysts maintained their cylindrical shape best, perhaps because of the swelling of internal cysts (Figs 3, 4). Although each data set encompassed almost all of the spinal cord segment (see Materials and methods), the mean numbers of sections in the spinal cord data sets were different in the three experimental groups. An average of 73.5 histological sections per spinal cord data set in the control group was used for three-dimensional reconstruction. The mean numbers of sections were 63.3 in the immediate PEG-treated and 54.3 in the delayed PEG-treated spinal cord
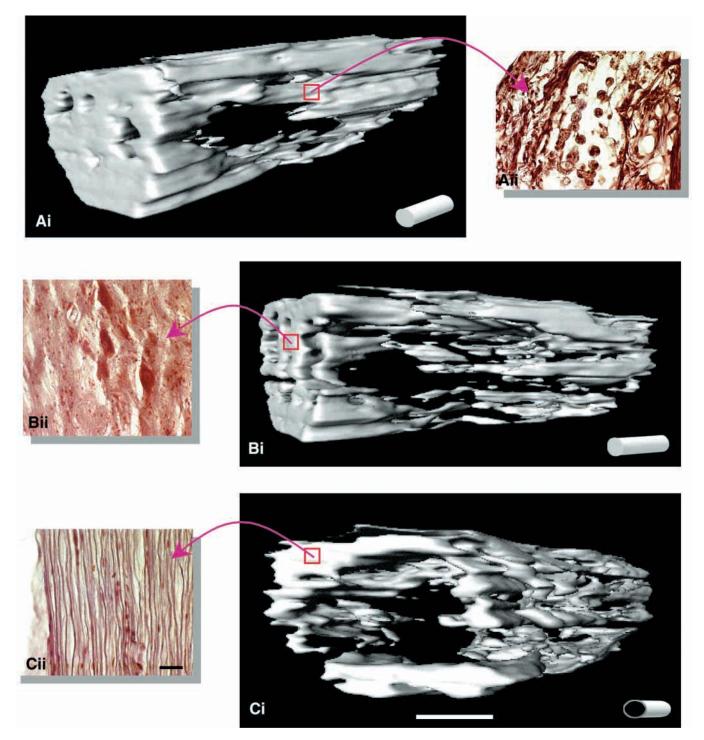
Fig. 4. Three-dimensional reconstruction of a control spinal cord segment. (Ai) A three-dimensional reconstruction of an entire 4.2 mm long spinal cord segment fenestrated by cysts. This image displays both normal and damaged spinal cord tissue with the cysts removed. One can see through this image because cystic cavitations transverse the width of the cord. Cysts can also be seen at the rostral end of the segment as pockets or invaginations at the end of the reconstructed spinal segment where these spaces (filled with fluid *in situ*) have extended beyond the boundary of the segment sectioned (refer to Fig. 2A). In Bi and Ci, only the undamaged parenchyma has been reconstructed. Aii shows cavitated and hemorrhagic gray matter inundated with macrophages (large circular cells in the center of the image). Bii shows a low-power photomicrograph of a region of partial sparing at the boundary of gray and white matter. Note the three well-stained neurons. Subpial sparing of white matter axons is shown in Cii. Note the orientation in Bi. In Ci, the spinal segment was rotated by approximately 200° in the horizontal plane. These reconstructions emphasize that intact parenchyma was mostly restricted to the periphery of the injured spinal segment and show the absence of contiguous gray and white matter through the lesion. The cylindrical icon gives the relative orientation of the three-dimensional segment; gray is the rostral end and black is the caudal end. Scale bars, 1 mm.
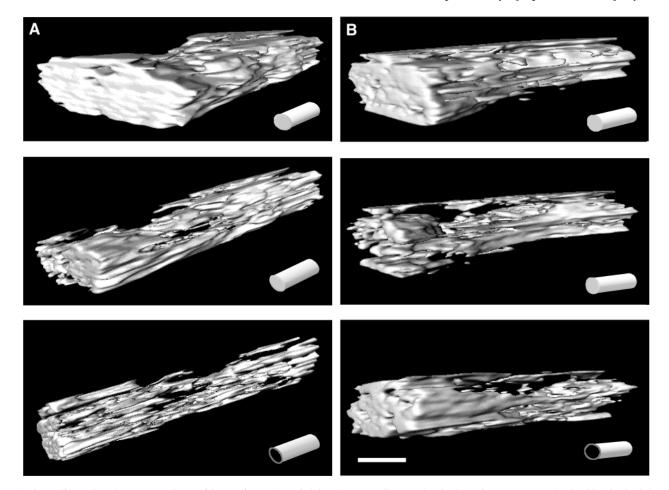
Fig. 5. Three-dimensional reconstructions of immediate (A) and delayed (B) PEG-treated spinal cord segments. In A, the histological data set was obtained from an animal to which PEG had been applied within 30 min of injury. (B) Three-dimensional reconstructions of a spinal cord segment for which application of PEG to the injury site was delayed for approximately 7 h. As in Fig. 4, the top images show both the normal and damaged parenchyma with the cysts removed from the image. Both spinal cord segments were markedly compressed at the epicenter of the compression injury. In the middle and bottom images, the intact parenchyma of the spinal segments is imaged. Bottom, the spinal segments have been rotated by approximately 180° in the horizontal plane from the middle image. These views emphasize the greater extent of contiguous gray and white matter through the lesions of PEG-treated cords compared with controls (see also Fig. 4). The cylindrical icon gives the relative orientation of the three-dimensional segment; gray is the rostral end and black is the caudal end. Scale bar, 1 mm

data set. This difference related to the relative stenosis of these cords, as discussed above, since the absolute volumes of the reconstructed spinal cord segments in each of the experimental groups were not statistically different ($P>0.05$).

The constant-displacement injury (Blight, 1991) (see also Borgens et al., 2002) produces a typical hemorrhagic lesion that destroys most of the central region of the spinal cord, usually sparing only a subpial rind of white matter. This was clearly evident since the thin bands of spared silver-impregnated axons were unmistakable, while more central columns and most gray matter were destroyed (see below). Fig. 2 shows typical histological sections at the lesion epicenter for untreated and PEG-treated spinal cord segments. The lesion area was centrally located at the region where the spinal cord was most compressed. In the untreated spinal cords, the lesion appeared less localized than in PEG-treated cords and surrounded the central cysts (Fig. 2). Fig. 2 also shows regions

of apparently normal parenchyma in untreated and PEG-treated spinal cords. This intact parenchyma in control segments was located mainly in the subpial region (surviving white matter) and was virtually non-existent at the lesion epicenter where these photomicrographs were obtained. This emphasizes the usefulness of the final reconstructed three-dimensional image, in which such sparing was easily observed (Figs 3, 4).

The three-dimensional reconstruction in Fig. 4 shows both the three-dimensional image and two-dimensional photomicrographs typical of regions of (i) destroyed central gray matter, (ii) marginal areas of spared gray and white matter and (iii) the subpial region of spared white matter. An evaluation of these images relative to the three-dimensional reconstructions provides the basis for the comparisons noted below. Surviving subpial regions were almost exclusively white matter; however, a thorough search revealed rare
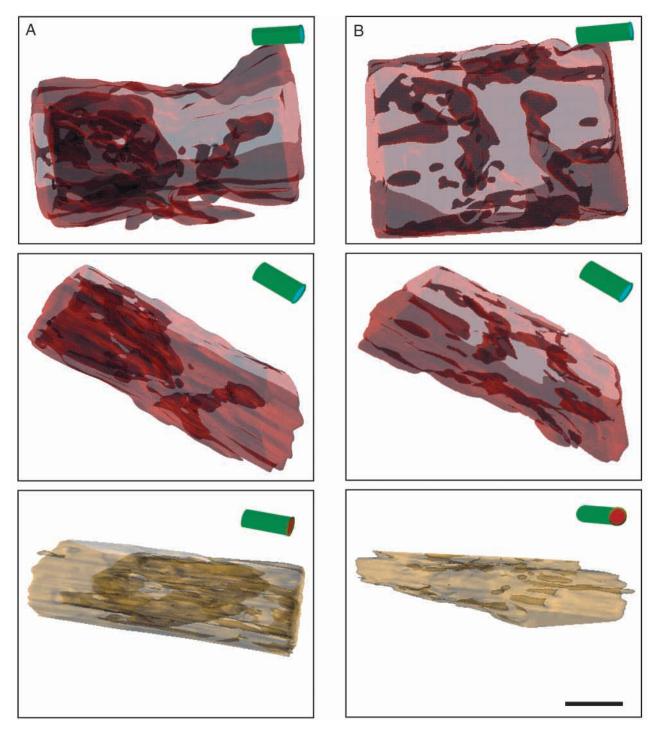
Fig. 6. Three-dimensional reconstruction of cavitation in control (A) and PEG-treated (B) spinal cord segments. In A, the dorsal surface of the spinal cord segment is facing the viewer; the ventral surface is towards the page. The surrounding tissues were made transparent, and the most dorsal surface of this spinal cord segment was also removed to provide an unobstructed view of the cysts (shown in dark red). (A) Top image, a large cystic cavity occupies the rostral (left) half of this segment. In the middle image, the spinal segment has been rotated vertically by approximately 90° so that the dorsal aspect is towards the top of the page, showing a side view of this extensive cavitation. Bottom image, a second sham-treated spinal cord segment shown for comparison. Note the similar, and very large, cyst in the center of the segment (colored brown). The ventral surface is facing the top of the page. (B) Top image, cysts were dispersed throughout the PEG-treated segment but mainly localized on either side of the site of injury. Middle image, this spinal segment has been rotated vertically so that the dorsal aspect is towards the top of the page, showing a side view of cavitation. Bottom image, an oblique side view of a second PEG-treated spinal cord segment; the dorsal surface is towards the top of the page. The embedded cysts are imaged in a darker color than the parenchyma surrounding them. These spinal cord reconstructions emphasize the markedly decreased amount of cavitation in PEG-treated cords compared with controls. In the orientation icon, red is the rostral end and blue is the caudal end. Scale bar, 1 mm.

examples of spared neurons (Fig. 4B) in regions of adjacent white matter and gray matter.

In PEG-treated spinal segments, normal-looking parenchyma (both gray and white) was more abundant than in untreated spinal cords (Figs 4, 5). The mean volume of normal-looking parenchyma after trauma in untreated spinal segments was 24.4 %, while 35.8 % of the nervous tissue survived after treatment in the immediate spinal cords and 49.7 % in delayed PEG-treated spinal cords (see Fig. 7A).

The amount of cavitation in these cords was the simplest pathological feature to discriminate between the groups (Figs 2, 6). In the PEG-treated spinal cord segments, the cysts were smaller and located on all sides of the central lesion (Figs 2B,D, 6B). In the sham-treated spinal cords, cysts were more prevalent throughout the entire length of the spinal cord segment (Figs 2A,C, 6A). Often cavitation was not contained within the field of view, extending beyond that segment of spinal cord (Figs 2–4). On average, 46.9 % of the total volume of the control spinal cord segment consisted of cysts compared with 32.4 % and 21.7 % for the immediate and delayed PEG-treated spinal cords, respectively (Fig. 7A).

Quantification of PEG-treated versus sham-treated spinal cord injuries

When the volume of cavitation was compared between groups, the control group was significant different from the immediate (*P*=0.002) and delayed (*P*=0.0001) PEG-treated groups. This was also true when the volume of intact parenchyma (mostly spared subpial white matter) in the control group was compared with the immediate (*P*=0.04) and delayed (*P*=0.02) PEG-treated groups. In addition, the volume of cavitation was greater in the immediate PEG-treated group than in the delayed PEG-treated group (*P*=0.0002) (Fig. 7A). The surface area of the lesion in both the immediate and delayed PEG-treated groups was also reduced compared with that of the control group (immediate PEG treatment, *P*=0.04; delayed PEG treatment, *P*=0.009) (Fig. 7B). The remainder of the comparisons were not statistically significant (*P*>0.05) (Fig. 7).

Using the normalized volume measurements derived from the control and PEG-treated groups, we performed correlation tests to determine whether there was a relationship between the sparing of parenchyma, the occurrence of cysts and the formation of the lesion. These tests resulted in high correlation coefficients between the amount of intact tissue and the size of the lesion in untreated (*r*=–0.81), immediate PEG-treated (*r*=–0.94) and delayed PEG-treated (*r*=–1.00) spinal cord segments (Fig. 8A). However, there did not appear to be a linear correlation between the volume of intact parenchyma and total cyst volume for untreated (*r*=–0.19), and immediate PEG-treated (*r*=0.57) groups (Fig. 8B). Correlation tests were also performed between cavitation and lesion size for control (*r*=–0.42), immediate PEG-treated (*r*=–0.81) and delayed PEG-treated (*r*=–0.86) groups (Fig. 8C). Only the correlation coefficient for the delayed PEG-treated group was statistically significant (*P*≤0.05).
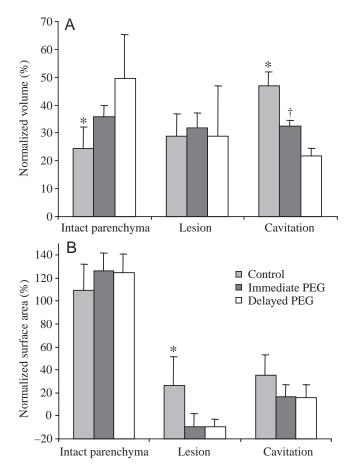

Fig. 7. Comparisons of volume and surface area measurements between untreated and PEG-treated spinal cords. (A) The normalized volume measurements for intact parenchyma, lesion and cystic cavities. The volume measurements for intact parenchyma and cavitation were statistically significantly different (asterisks) between the control group and both PEG-treated groups. (B) The normalized surface area measurements for the same groups. The surface area measurements for lesions were statistically significantly different between the control group and both PEG-treated groups. There was a statistically significant difference in the amount of cavitation between the immediate and delayed PEG-treated groups. Values are means + S.D. *Indicates a significant difference between control and experimental spinal cords (*P*<0.05; unpaired Student's *t*-test). †Indicates a significant difference between immediate and delayed PEG-treated spinal cords (*P*<0.05; unpaired Student's *t*-test).
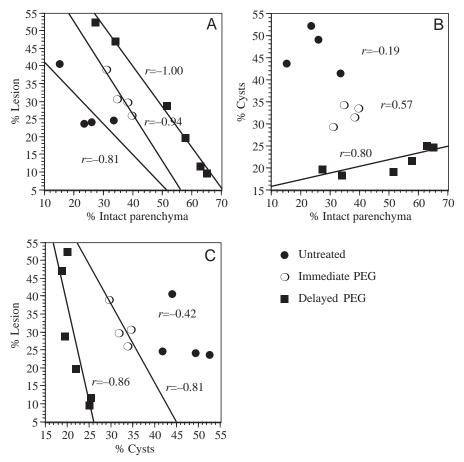
Discussion

We have used three-dimensional surface reconstruction techniques to compare the three-dimensional shape, volume and pathological character of lesions produced by compression injury to the spinal cord between PEG-treated and untreated guinea pigs. The spinal cords treated with PEG were separated into two groups, one in which the polymer was applied immediately after injury and a second in which the application was delayed for approximately 7 h. Both treated groups showed a marked increase in the volume of intact parenchyma and a reduction in the amount of cystic cavitation compared with untreated animals. Moreover, the lesion in PEG-treated

Fig. 8. Correlation tests between the volume of intact spinal cord tissue, cavitation and the lesion. Pearson correlation tests were performed to determine whether there were linear relationships between the volume percentages of intact parenchyma, lesion and cavitation. (A) There appears to be a strong inverse relationship between the volume of intact nervous tissue and the volume of lesion in the untreated control group and in the immediate and delayed PEG-treated groups. Thus, an increase in the volume of spinal cord sparing translates into a decrease in lesion formation. (B) A correlation between the volumes of undamaged tissue and the volume of cysts was observed only in the delayed PEG-treated group. (C) The amount of cavitation appears to be related to the amount of lesion being formed in the experimental spinal cords. Note that the correlation test for only the delayed PEG-treated group was statistically significant ($P \leq 0.05$).

animals was more focal and less diffuse within the injured segment of spinal cord, as emphasized by the statistically significant increase in the surface area of control lesions. Thus, a brief application of PEG can strikingly affect both the size and shape of the injury and the character of pathological cavitation.

Three-dimensional methodology

We believe that the use of every histological section comprising the data set for each spinal cord during three-dimensional reconstruction, the absence of human interaction in the gathering of data and the precise quantitative querying of the three-dimensional model produced reliable visualizations and numerical data for comparison. The anatomical structures of the injured spinal cord segments that we imaged and quantified were delineated on pixel value differences in the histological image. This eliminated the subjective method of identification of anatomy as well as the widespread manual tracing of structures of interest by an investigator prior to three-dimensional reconstruction and quantification. These differences in pixel values were based on the very different staining characteristics of intact and destroyed gray and white matter and the absence of staining that revealed cysts in relief. This approach is less biased and more precise than other three-dimensional reconstruction methods applied to spinal cord injury that require manual

tracing of regions of interest for each section and the morphing of regions of spinal tissue between the relatively few histological sections used to produce the three-dimensional model. In many such studies, only one histological section in ten is registered and imaged, producing a visualization that is questionably 90 % computer-extrapolated (Halliday et al., 1993; Martone et al., 1993; Navarro et al., 1994; Liss, 1995; Beattie et al., 1997). We have reviewed and compared several three-dimensional reconstruction methods, including the algorithm used here, with others in the literature (Moriarty et al., 1998; Duerstock et al., 2000).

The three-dimensionally reconstructed injury

Because of the severity of the compression injury, the overall damage to the spinal cords was very pronounced. Cavitation in most animals was especially prevalent. We found that cavitation in the untreated spinal cords was significantly greater than in the PEG-treated groups. In the control spinal cords, cysts usually extended throughout most of the cross-sectional area of the spinal cord segment and beyond. Thus, the quantification of cysts was very conservative, underestimating their size, which subsequent to correction would have increased the statistical difference between controls and experimentals.

The total number of histological sections per data set varied

among the spinal cord segments that we reconstructed three-dimensionally. The difference in the number of sections between control and delayed PEG-treated spinal cords resulted from their different pathologies rather than from differences in histological preparation. In all three-dimensional reconstructions, the entirety of the injury site was contained within the data set of histological sections. The control cords were more cavitated than the experimental cords and, in some cases, cysts extended out of the section in the rostral/caudal direction. Curiously, it appears that cysts generally helped maintain the roughly cylindrical shape of the spinal cord better than in less cavitated PEG-treated cords. This may have been because cysts increased the turgidity of the spinal segment by a 'ballooning' effect, producing a larger-diameter segment to be histologically sectioned (Figs 2–4). In contrast, the PEG-treated spinal cord segments tended to form a compact hourglass shape requiring less sectioning to produce a complete data set (see Figs 2–5). Indeed, although the PEG-treated spinal segments were smaller in diameter, they contained a greater absolute volume of both intact and damaged nerve tissue than the control spinal cord segments.

Intact regions of both white and gray matter were also more prevalent in PEG-treated cords. We emphasize that, while spared parenchyma was not exclusively white matter (see Fig. 4B), examples of surviving neurons in gray matter was rare. This is due to the centrifugal spread of tissue loss during 'central hemorrhagic necrosis', since gray matter is richly vascularized (Allen, 1911), and the centralized focus of force when a cylinder of a sol/gel (i.e. spinal cord) is impacted from the outside. Nonetheless, the overall lesion was smaller in PEG-treated cords than in controls. This suggests that PEG may also seal damaged neuronal (and other cell body) membranes in addition to their processes. This has been directly tested *in vitro* using a related polymer, Poloxamer 188. Application of this triblock (polyethylene–polypropylene–polyethylene) polymer provided potent neuroprotection to hippocampal and cerebellar neurons in culture exposed to oxidative and excitoxic injury (Marks et al., 2001). PEG-mediated sparing in dorsal regions of white matter probably contributed to the striking recovery of somatosensory evoked potential conduction following tibial nerve stimulation relative to a complete lack of such conduction in control animals (Borgens et al., 2002; Borgens and Shi, 2000).

The lesion itself was another structure of interest. Damaged or destroyed spinal cord parenchyma was largely devoid of silver-stained neurons or their processes, appearing pale red in comparison. In PEG-treated spinal cords, the lesion was localized in the center of the site of injury. In untreated spinal cords, the lesion was less localized and was spread diffusely throughout the entire spinal segment surrounding the more numerous cysts. This observation was supported by measurements of the extended surface area of the lesion in control cords relative to treated cords.

Three-dimensional quantification

There was a statistically significant decrease in the surface area of the lesion in PEG-treated spinal segments compared with untreated spinal segments, as discussed above. The volume of intact spinal cord parenchyma was found to be significantly greater in PEG-treated animals than in untreated animals, while the volume of cavitation was significantly smaller. The application of PEG to compressed spinal cords may have resulted in the rescue of compromised cells, leading to a reduction in the spread of cavitation.

We investigated whether the lesion and cysts in PEG-treated and untreated spinal cords were related to the amount of spared parenchyma. It appeared that an increased amount of intact spinal cord tended to be correlated to a decrease in the size of the lesion in experimental and control groups, as one might expect. This was definitely true for delayed PEG-treated animals, for which regression analysis resulted in markedly statistically significant correlation coefficients ($P=0.0001$; see Fig. 8A). However, no direct relationship was evident between the volume of intact parenchyma and the volume of cysts that formed within injured spinal cords, except in the delayed PEG-treated group (Fig. 8B).

We have not shown conclusively that, with increasing cavitation, lesion formation decreased, although a trend in this direction occurred in the PEG-treated groups (Fig. 8C). For the delayed PEG-treated animals, the correlation test proved statistically significant ($P=0.03$). In control spinal cords, the process of cavitation did not appear to be directly related to the volume of the lesion. Although cell death and the resultant inflammatory reaction may initiate cavitation, there are certainly other factors that control its extent (see Perry et al., 1987, 1993; Leskovar et al., 2000).

Finally, these data provide insight into the gross anatomical effects of a brief PEG treatment to the compression-injured spinal cord. In addition to (i) a very rapid and measurable recovery of physiological and behavioral function (Borgens and Shi, 2000; Borgens et al., 2002), (ii) a rapid sealing of membrane breaches to individual axons within white matter revealed by a dye-exclusion test (Shi and Borgens, 2001), we can add (iii) that the total amount of intact parenchyma is augmented and (iv) that the extent of cystic cavitation is significantly reduced by PEG treatment.

References

Allen, A. R. (1911). Surgery of experimental lesions of spinal cord equivalent to crush injury of fracture disk location. *J. Am. Med. Ass.* **57**, 878–888.

Arndt, S., Swayze, V., Cizadlo, T., O'Leary, D., Cohen, G., Yuh, W. T. C., Ehrhardt, J. C. and Andreasen, N. C. (1994). Evaluating and validating two methods for estimating brain structure volumes: Tessellation and simple pixel counting. *Neuroimage* **1**, 191–198.

Bajaj, C. L., Pascucci, V. and Schikore, D. R. (1997). The contour spectrum. In *Proceedings of the IEEE Visualization 1997 Conference* (ed. R. Yagel and H. Hagen), pp. 167–175. ACM Press.

Beattie, M. S., Bresnahan, J. C., Komon, J., Tovar, C. A., Van Meter, M., Anderson, D. K., Faden, A. I., Hsu, C. Y., Noble, L. J., Salzman, S. and Young, W. (1997). Endogenous repair after spinal cord contusion injuries in the rat. *Exp. Neurol.* **148**, 453–463.

Blight, A. R. (1985). Delayed demyelination and macrophage invasion: A candidate for secondary cell damage in spinal cord injury. *Centr. Nervous Syst. Trauma* **2**, 299–315.

Blight, A. R. (1991). Morphometric analysis of a model of spinal cord injury in guinea pigs, with behavioral evidence of delayed secondary pathology. *J. Neurol. Sci.* **103**, 156–171.

Blight, A. R. (1992). Macrophages and inflammatory damage in spinal cord injury. *J. Neurotrauma* **9**, s83–s91.

Blight, A. R. (1993). Remyelination, revascularization and recovery of function in experimental spinal cord injury. In *Advances in Neurobiology: Neural Injury and Regeneration*, vol. 59 (ed. F. J. Seil), pp. 91–103.

Borgens, R. B. and Shi, R. (2000). Immediate recovery from spinal cord injury through molecular repair of nerve membranes with polyethylene glycol. *FASEB J.* **14**, 27–35.

Borgens, R. B., Shi, R. and Bohnert, D. (2002). Behavioral recovery from spinal cord injury following delayed application of polyethylene glycol. *J. Exp. Biol.* **205**, 1–12.

Bresnahan, J. C., Beattie, M. S., Stokes, B. T. and Conway, K. M. (1991). Three-dimensional computer-assisted analysis of graded contusion lesions in the spinal cord of the rat. *J. Neurotrauma* **8**, 91–97.

Davison, R. I., O'Malley, K. A. and Wheeler, T. B. (1976). Polyethylene-glycol-induced mammalian cell hybridization: effect of polyethylene glycol molecular weight and concentration. *Somat. Cell Mol. Genet.* **2**, 271–280.

Duerstock, B. S., Bajaj, C. L., Pascucci, V., Schikore, D., Lin, K.-N. and Borgens, R. B. (2000). Advances in three-dimensional reconstructions of the experimental spinal cord injury. *Comput. Med. Im. Grap.* **24**, 389–406.

Halliday, G. M., Cullen, K. and Cairns, M. J. (1993). Quantitation and three-dimensional reconstruction of Ch4 nucleus in the human basal forebrain. *Synapse* **15**, 1–16.

Harris, K. and Stevens, J. K. (1988). Dendritic spines of rat cerebellar Purkinje cells: Serial electron microscopy with reference to their biophysical characteristics. *Neuroscience* **8**, 4455–4469.

Hashimoto, S. and Kimura, R. S. (1988). Computer-aided three-dimensional reconstruction and morphometry of the outer hair cells of the Guinea Pig cochlea. *Acta Otolaryngol.* **105**, 64–74.

Honmou, O. and Young, W. (1995). Traumatic injury to the spinal axons. In *The Axon* (ed. S. G. Waxman, J. D. Kocsis and P. K. Stys), pp. 480–503. New York: Oxford University Press.

Krause, T. L. and Bittner, G. D. (1990). Rapid morphological fusion of severed myelinated axons by polyethlene glycol. *Proc. Natl. Acad. Sci. USA* **87**, 1471–1475.

Lee, J. and Lentz, B. R. (1997). Evolution of lipidic structures during model membrane fusion and the relation of this process to cell membrane fusion. *Biochemistry* **36**, 6251–6259.

Leskovar, A., Moriarty, L., Turek, J. J., Schoenlein, I. A. and Borgens, R. B. (2000). The macrophage in acute neural injury: changes in cell numbers over time and levels of cytokine production in mammalian central and peripheral nervous system. *J. Exp. Biol.* **203**, 1783–1795.

Liss, A. G. (1995). Computer-assisted method for simultaneous three-dimensional reconstruction of highly magnified nerve endings and low-magnification contours of the spinal cord. *J. Microsc.* **178**, 160–164.

Marks, J. D., Pan, C.-Y., Bushell, T., Cromie, W. and Lee, R. C. (2001). Amphiphilic, triblock polymers provide potent, membrane-targeted neuroprotection. *FASEB J.* (in press).

Martone, M. E., Zhang, Y., Simpliciano, V. M., Carragher, B. O. and Ellisman, M. H. (1993). Three-dimensional visualization of the smooth endoplasmic reticulum in Purkinje cell dendrites. *J. Neurosci.* **13**, 4636–4646.

Moriarty, L. J., Duerstock, B. S., Bajaj, C. L., Lin, K. and Borgens, R. B. (1998). Two- and three-dimensional computer graphic evaluation of the subacute spinal cord injury. *J. Neurosci.* **155**, 121–137.

Nakajima, N. and Ikada, Y. (1994). Fusogenic activity of various water-soluble polymers. *J. Biomater. Sci. Polym. Ed.* **6**, 751–759.

Navarro, A., Tolivia, J. and Alvarez-Uría, M. (1994). Hamster supraoptic nucleus: cytoarchitectural morphometric and three-dimensional reconstruction. *Anat. Rec.* **240**, 572–578.

Noble, L. and Wrathall, J. (1985). Spinal cord contusion in the rat: morphometric analyses of alterations in the spinal cord. *Exp. Neurol.* **88**, 135–149.

O'Lague, P. H. and Huttner, S. L. (1980). Physiological and morphological studies of rat pheochromocytoma cells (PC12) chemically fused and grown in culture. *Proc. Natl. Acad. Sci. USA* **77**, 1701–1705.

Perry, V. H., Andersson, P. B. and Gordon, S. (1993). Macrophages and inflammation in the central nervous system. *Trends Neurosci.* **16**, 268–273.

Perry, V. H., Brown, M. C. and Gordon, S. (1987). The macrophage response to central and peripheral nerve injury: a possible role for macrophages in regeneration. *J. Exp. Med.* **165**, 1218–1223.

Salisbury, J. R. (1994). Three-dimensional reconstruction in microscopical morphology (Invited Review). *Histol. Histopathol.* **9**, 773–780.

Shi, R. and Borgens, R. B. (1999). Acute repair of crushed guinea pig spinal cord with polyethylene glycol. *J. Neurophysiol.* **81**, 2406–2414.

Shi, R., Borgens, R. B. and Blight, A. R. (1999). Functional reconnection of severed mammalian spinal cord axons with polyethylene glycol. *J. Neurotrauma* **16**, 727–738.